International Journal of
INTELLIGENT SYSTEMS AND APPLICATIONS IN ENGINEERING

ISSN:2147-6799 www.ijisae.org Original Research Paper

Multi-Class Classification of Skin Cancer Using Hybrid Inception-Residual Network

Ayoobkhan Mohamed Uvaze Ahamed[1], Venkata Rajesh Yella[2], Dr. P. Vamsi Krishna[3], Subramanian M.[4], Dr. Amar Kumar Dey[5], Santosh Kumar Behera[6]

Submitted: 19/09/2023 **Revised**: 18/11/2023 **Accepted**: 29/11/2023

Abstract: Due to the emergence of medical applications, skin cancer is considered as one of the most common types of disease. Though, the occurrence of melanoma is seen in the form of cancer, it is complex to predict. When the lesions are found in the early phases, the survival rate of the patient may be increased. But, the existing automated models highly rely on the hand-crafted features and it is a complex process. Hence, this work aims to detect the multi-class of skin cancer using a deep learning (DL) model. The major processes like hair removal, optimal segmentation, feature extraction and classification processes are carried out. Initially, the hair removal process is carried out in the pre-processing stage. Then, for segmenting the affected region, optimal fuzzy clustering (OFC) is carried out. Finally, the enhanced DL model hybrid Inception-Residual network (Hybrid I-R network) is used for extracting and classifying the three stages of skin cancer. The Hybrid I-R network is the integration of an Inception-Residual network and dense network. The overall evaluation is carried out on the ISIC dataset and 5-fold cross-validation is carried out. The performances of the proposed hybrid model are compared with the other existing models and achieved better accuracy, recall and precision of 99.78%, 99.12% and 98.9% respectively. This shows that this model is more robust and reliable and efficiently utilized in skin cancer classification.

Keywords: *Skin Cancer, Medical Applications, Deep Learning, Data-Augmentation, Classification*

1. Introduction

In the world, skin cancer is considered as one of the fast growing diseases and it mainly occurs due to the ultra-violet radiation [1]. There are four types of skin cancer; they are Melanoma, solar keratoses, Basal cell carcinoma (BCC), and Squamous cell carcinoma (SCC). Melanoma is one kind of malignancy that initiates from melanocytes located in the epidermis of skin [2-5]. When compared to Squamous cell carcinoma and solar keratosis, melanoma is the most harmful one. According to the report of the dermatologist, when melanoma is identified in the initial stages, there is a 95% feasibility of curing it [6]. Human skin has three types of tissues like dermis, hypodermis and epidermis. The epidermis ha melanocyte and it produces melanin at a high rate. The abnormal growth of melanocytes develops melanoma.

[1]*Software Engineering, New Uzbekistan University, Tashkent, Uzbekistan, uvazeahamedphd@yahoo.com*

[2]*Assistant Professor, Department of Biotechnology, KoneruLakshmaiah Education Foundation, Green Fields, Vaddeswaram, Guntur, Andhra Pradesh, India, yvrajesh_bt@kluniversity.in*

[3]*Assistant Professor, School of Management, Malla Reddy University, Hyderabad, Telangana, India, vamsi.pratapa@yahoo.co.in*

[4]*Assistant Professor, Department of Electronics and Instrumentation Engineering,Sai Leo Nagar,West Tambaram,Chennai, Tamilnadu, India, subramanian.ei@sairam.edu.in*

[5]*Assistant Professor, Department of Electronics and Telecommunications Engineering, Bhilai Institute of Technology, Durg (C.G), India, amardeyhope@gmail.com*

[6]*Lecturer, JeyporeCollege of Pharmacy, Jeypore, Odisha, India, santoshbehera696@gmail.com*

According to the report of the world health organization (WHO), skin cancer is the third leading cause of death. In the United States, nearly 5.6 million people are affected due to this disease. In Europe, nearly 1 lakhs melanoma affected people are reported per year. Treatment and skin cancer detection are traditionally performed by visual inspection and manual analysis and biopsy. This manual detection by dermatologists are error prone, time consuming and complex. This is because of the complicated nature of skin cancer images [7]. Even though, the biopsy is one of the easiest models for diagnosing cancer; however the procedure is unreliable and complex. Recently, non-invasive devices help assist dermatologists use dermoscopic and macroscopic images. The dermoscopic images have high resolution and it is obtained from deep skin structures visualization. Generally, macroscopic images have less resolution and quality since they are obtained by mobiles and cameras [8-11].

The early diagnosis of skin cancer may increase the survival rate of the patients. The major challenge of dermoscopy is the need for extended training. In the last two decades, various kinds of computer aided diagnosis (CAD) models are introduced for identifying skin cancer [12]. CAD models assist in extracting more useful features from the images. Generally, CAD model has the stages like pre-processing, segmentation, extraction of features and classification. Every process has a significant impact on the performance of the entire CAD model [6]. Hence, an efficient model must be used in every process for achieving better performance in diagnosis.

Recently, the artificial intelligence (AI) has been widely utilized in disease diagnosis. Traditionally, the computer vision models are mainly utilized as the classifier for extracting more features like shape, texture, size and color for detecting cancer [13]. This type of machine learning (ML) needs more time for the accurate detection. Further, their performance is based on the features selected that show the lesions parts [14]. The traditional classification models used for the skin cancer are artificial neural network (ANN), K-nearest neighbor (KNN) and support vector machine (SVM). Recently, the deep learning (DL) models have shown remarkable success in the analysis of skin cancer. The DL models like deep neural network (DNN), convolutional neural network (CNN), ResNet, long short term memory (LSTM) and InceptionNet are used in the healthcare field for detecting the cancer cell [15]. The existing research works failed to classify the multi-classes in skin disease classification. The major objectives of the research are:

- To introduce various pre-processing and segmentation procedures for improving the training performance.
- To carry out the optimal segmentation using fuzzy C means clustering (FCM) with enhanced squirrel search optimization (ESSO).
- To introduce a hybrid Inception-Residual network (Hybrid I-R network) for extracting and classifying the three stages of skin cancer.
- To validate the performance of the proposed hybrid model with other models on the ISIC dataset.

The rest of the research work is sorted as follows: Section 2 is the recent related works based on skin cancer disease classification. Section 3 presents the proposed skin cancer disease classification with the mathematical description, Section 4 is the results and discussions, and the entire work is concluded in Section 5.

2. Related Works

Some of the recent research work is discussed in this section with their performance achievements.

Chaturvedi et al. [16] presented an automated MCSC (multi-class skin classification) using five pre-trained CNNs and four ensemble approaches. The experimentation was carried out on the HAM10000 dataset and achieved better accuracy of 93% for the individual approaches and better accuracy of 92.8% for the ensemble approach. Finally, it was concluded that ResNeXt101 was more suitable for MCSC because of its optimized model and ability to attain better accuracy.

Ali et al. [17] presented an enhanced model for the classification of skin cancer using DCNN with transfer learning (TL) models. Initially, the filtering was applied for removing noise, the images were normalized and features were extracted. Finally, data augmentation process was used for increasing the classification accuracy. This model was carried out on HAM10000 dataset and achieved higher accuracy of 93.1%.

Sedigh et al. [18] presented the CNN model for detecting skin cancer on the ISIC dataset. Then, for compensating the lack of data during the training process, the DL model GAN (Generative Adversarial Networks) was used for producing the synthetic images. The experimentation was carried out with and without synthetic images and achieved better accuracy of 71% (with synthetic images) and 53% (without synthetic images).

Garg et al. [19] presented a decision support model to detect and classify skin cancer using the HAM-10000 dataset. The major aim of the work was to identify skin cancer and classify the various stages using CNN. The noise was removed and image resolution was enhanced and the image count was enhanced by the image augmentation process. Finally, transfer learning (TL) was used for increasing the accuracy in classification. This model achieved better F1 and precision of about 0.77 and 0.88 respectively.

Kumar et al. [20] presented a differential evolution (DE) based ANN model for the detection of skin cancer. Initially, different filters were utilized for enhancing the image attributes. Then, the color and texture features were extracted and classified. The experimentation was carried out on PH2 and HAM-10000 datasets. This model achieved better accuracy and sensitivity of 97.4% and 90%.

Mijwil [21] presented three DL models like VGG19, ResNet and InceptionNet models to classify the cancer as malignant or benign. The performance was carried out on ISIC dataset and the InceptionV3 model was considered the best model. This model achieved better accuracy and precision of 86.9% and 87.4%. Zhang et al. [22] presented a diagnosis of skin cancer on the basis of optimized CNN. Then, the Levy flight based whale optimization algorithm was used for optimizing the weights of CNN. The experimentation was carried out on the Dermquest dataset and applied ten different models. This model proved that this model segmented the lesions and also detected lesions with artifacts.

Amin et al. [23] presented deep features to localize and classify the skin cancer. Initially, the images were resized; bi-orthogonal wavelet and Otsu were used for segmenting the images. Then the DL models like

VGG16 and AlexNet were fused and the features were selected by PCA (Principle Component Analysis) and benign and malignant classes were classified. Afza et al. [24] presented the hybrid feature selection and classification using ELM (extreme learning machine). Here, the input images were enhanced and the features were selected using whale optimizer. Finally, ELM was used for classification and the experimental results were evaluated on the ISIC and HAM10000 datasets.

Raju et al. [26] presented clustering based model for skin disease classification. Here, the skin diseases like paederus, melanoma, benign, herpes and psoriasis were considered. The lesions were segmented using the fuzzy-set model. Then, the color, shape and texture features were extracted. Finally, the SVM with BWO (black widow optimization) was used for classifying the lesions. The experimental analysis was carried out in the ISIC-2018 dataset and achieved better accuracy of 92%.

Karthik et al. [27] developed EfficientNetV2 with ECA (Efficient Channel Attention) for the skin cancer diagnosis. Here, the lesions like melanoma, psoriasis, acne and actinic were classified. This existing model analyzed approximately 16M variables for classifying the disease and the overall accuracy achieved was 84.7%.

Melbin et al. [28] developed automatic skin disease classification by diverse features and IGWO (improved grey wolf optimizer). For segmenting the lesions, circular kernel and morphological operations were carried out. The features were extracted by ABCD (asymmetry, border, color and differential structures). Finally, the SVM was utilized for classification and achieved the accuracy of 97%.

It is observed from the existing works that most of works were relied on the hand-crafted features like GLCM and LBP. Further, the segmentation using the clustering and conventional segmentation approaches is not efficient in segmenting the lesions. Hence, there is a need of approach which provides optimal segmentation and classification of images with relying on the hand-crafted features.

3. Proposed Methodology

Melanoma is one kind of skin disease and it can be treated when it is identified in the initial stage. This research work aims to provide a multi-class skin cancer detection model which enhances the accuracy and speed of the diagnosis. The following section shows the working process of the proposed skin cancer classification model. In this work, the CAD based DL model is used for the automatic lesion classification. The major aim of the work is to extract and classifies the three stages of cancer on the benchmark ISIC 2019 dataset. Figure 1 represents the architecture of the proposed multi-skin cancer classification model. Here, initially, input images are acquired from the ISIC dataset, and then the hair removal process is carried out in the pre-processing. Finally the optimal segmentation is carried out by FCM-ESSO and the features are extracted and classified using HDIRN.

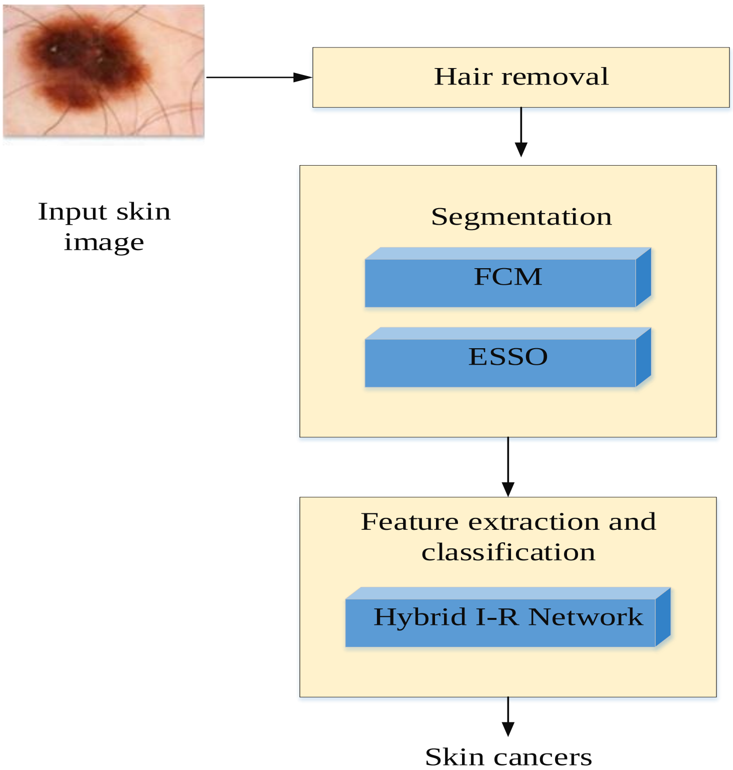

Fig 1: Architecture of the proposed multi-skin cancer classification model

3.1 Dataset acquisition

The dataset utilized in this work is obtained from the ISIC 2019 [25] (International Skin Imaging Collaboration) from the Kaggle website. In this work, 25331 images of 8 classes are utilized. They are BCC, AK (actinic keratosis), BK (benign keratosis), melanoma, vascular lesion (VL), SCC and MN (melanocytic nervus). The sample images of ISIC 2019 dataset are given in Figure 2.

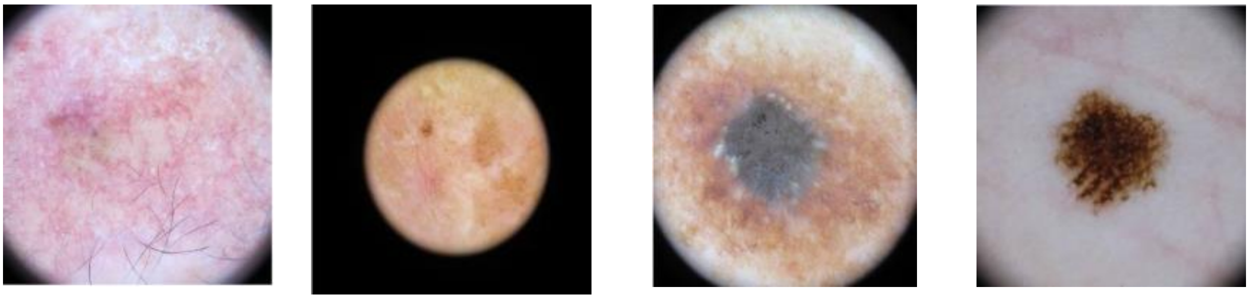

BCC AK BK melanoma

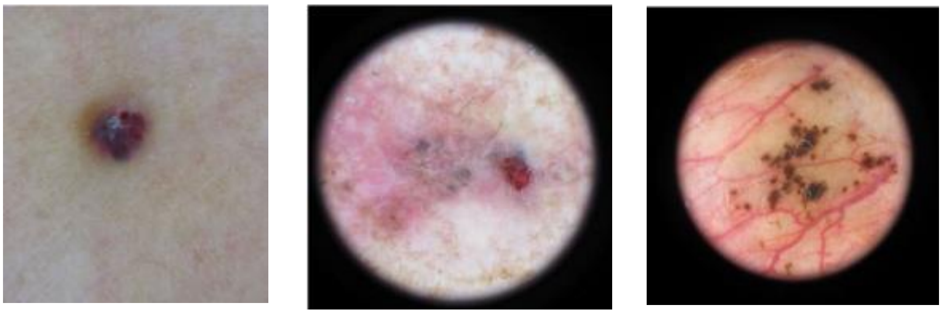

VL SCC MN

Fig 2: Sample images of ISIC 2019 dataset

3.2Pre-processing

The pre-processing of the images is the essential stage when dealing with complicated skin images. Initially, the hair removal process is used to remove hair from the skin images. The input RBG images are converted into grayscale image and morphological blackhat operation is performed. It is used for increasing the skin lesion images that have fine hair which is darker that the surface and lighter that the structured element. Then the fine hair contour's intensity is improved by thresholding image. Finally, a clear image without the hair is obtained and it is given in Figure 3.

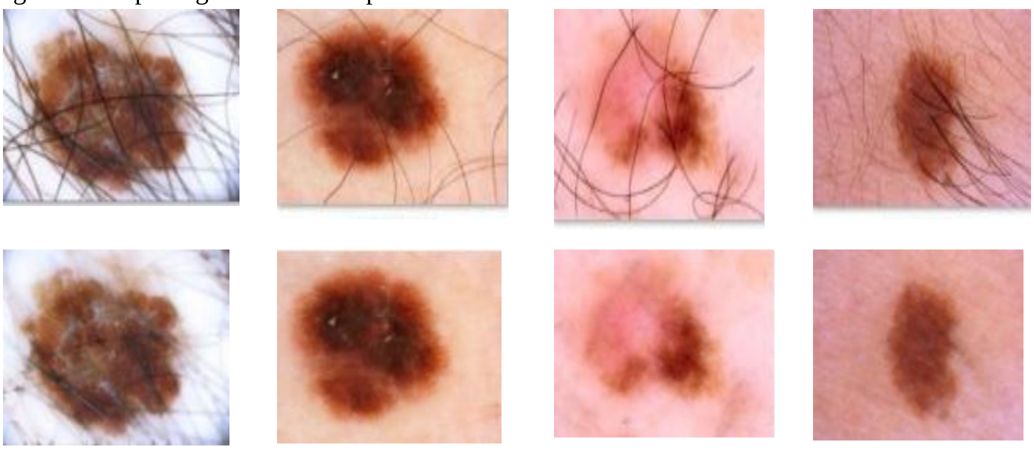

Fig 3: Hair removal process in the ISIC dataset

3.3 Optimal segmentation

In this work, for segmenting the skin lesions, optimal clustering process is carried out FCM. Here, the optimal cluster centers are identified by the ESSO.

FCM: The FCM is unsupervised clustering and here every data points M show the single partition. The cluster centers d_l are computed by:

$$d_l = \frac{\sum_{m=1}^{N} v_{l,i}^{n}, y_i}{\sum_{m=1}^{N} v_{l,i}^{n}} \qquad (1)$$

where n is the number of fuzziness, $v_{l,i}$ is the degree of pixel membership and is represented as:

$$v_{l,i} = \frac{1}{\sum_{L=1} \frac{c_{l,i}^{2/n-1}}{c_{l,i}}} \qquad (2)$$

where $c_{l,i}$ is the i^{th} cluster in the l^{th} pixel.

ESSO begins with the randomized initial position of flying squirrels (F_s) and its position is indicated using the vector in the dimensional space $(\dim)$. Thus, the F_s can slide in 1D, 2D and 3D space. The mathematical representation of the weight updation using ESSO is discussed in the following section:

Random initialization: let us consider m number of F_s in forest and position of j^{th} F_s is represented using the vector. The position of every F_s is indicated by the below matrix:

$$F_s = \begin{bmatrix} F_{s1,1} & F_{s1,2} & \cdots & \cdots & F_{s1,\dim} \\ F_{s2,1} & F_{s2,2} & \cdots & \cdots & F_{s2,\dim} \\ \vdots & \vdots & \vdots & \vdots & \vdots \\ \vdots & \vdots & \vdots & \vdots & \vdots \\ F_{sm,1} & F_{sm,2} & \cdots & \cdots & F_{sm,\dim} \end{bmatrix} \qquad (3)$$

An uniform distribution is utilized for allocating the initial position of every F_s in forest and it is given as:

$$F_{sj} = F_{sl} + U(0,1) \times (F_{su} - F_{sl}) \qquad (4)$$

where F_{sl} and F_{su} are the lower and upper limits of j^{th} F_s.

Evaluating fitness: The fitness of position for every F_s is computed using solution vector into the fitness function of user.

$$f = \begin{bmatrix} f_1([F_{s1,1} \; F_{s1,2} & \cdots & \cdots & F_{s1,\dim}]) \\ f_2([F_{s2,1} \; F_{s2,2} & \cdots & \cdots & F_{s2,\dim}]) \\ \vdots \quad \vdots & \vdots & \vdots & \vdots \\ \vdots \quad \vdots & \vdots & \vdots & \vdots \\ f_m([F_{sm,1} \; F_{sm,2} & \cdots & \cdots & F_{sm,\dim}]) \end{bmatrix}$$

(5)

Generating new positions: there are three stages happen during the foraging of F_s. In every situation, it is considered that without predator, F_s slide and find effectively over the forest for the likely food. However, the predator's presence creates it careful and is forced to search the hiding position. These three stages are mathematically given as:

Stage 1: F_s which are on oaknut trees F_{sot} move to hickory tree F_{sht}^{t}. In this stage, the new position of squirrels is given as:

$$F_{sot}^{t+1} = \begin{cases} F_{sot}^{t} + d_s \times S_c \left(F_{sht}^{t+1} - F_{sot}^{t} \right) & Rand1 > P_{pr} \\ random\ \ position & elsewhere \end{cases}$$

(6)

where d_s is the random sliding distance, S_c gliding constant, $Rand1$ is the random number and P_{pr} is the probability of predator.

Stage 2: F_s which are on normal trees F_{snt} move to F_{sot} for fulfilling the regular energy requirements. In this stage, the new position of squirrels is indicated as:

$$F_{snt}^{t+1} = \begin{cases} F_{snt}^{t} + d_s \times S_c \left(F_{sot}^{t+1} - F_{snt}^{t} \right) & Rand2 \geq P_{pr} \\ random\ \ position & elsewhere \end{cases}$$

(7)

Where $Rand2$ is the random number.

Stage 3: The squirrels on the F_{snt} and already consumed F_{sot} move to F_{sht}^{t} for storing the nuts in hickory and it is represented by:

$$F_{snt}^{t+1} = \begin{cases} F_{snt}^{t} + d_s \times S_c \left(F_{sht}^{t+1} - F_{snt}^{t} \right) & Rand3 \geq P_{pr} \\ random\ \ position & elsewhere \end{cases}$$

(8)

Where $Rand3$ is the random number.

Flight of sliding: The sliding of F_s is estimated using equilibrium slide in which total of lifting L and dragging D generates the resulting force R. It is represented as:

$$\frac{L}{D} = \frac{1}{\tan\theta} \qquad (9)$$

Relocating to new area: For enhancing the exploration capacity of the optimizer, the random relocation of some F_s which are not explored the optimized food source. It is given as:

$$F_{snt} = F_{sl} + Levy(n)(F_{su} - F_{sl}) \qquad (10)$$

where $Levy(n)$ is the levy's flight operation utilized to explore the search space, F_{su} and F_{sl} are the upper and lower limits. In this work for enhancing the exploitation capacity of the optimizer, the improved predator is included and it is expressed as:

$$P_{pr} = (P_{pr\max} - P_{pr\min})\left(1 - \frac{Iter}{Iter\max}\right)^{10} + P_{pr\max} \qquad (11)$$

where $P_{pr\max}$ and $P_{pr\min}$ are the maximum and minimum value of improved predator. Algorithm 1 defines the pseudocode for segmentation using FCM-ESSO.

Algorithm 1: Pseudocode for segmentation using FCM-ESSO
Input: pre-processed images, n and number of cluster
Output: Optimal cluster centers
Identify d_l and $v_{l,i}$ using Equations (1) and (2)
initial position of every F_s in forest is identify by Equation (4)
Evaluating fitness using Equation (5)
while $t < \max\_iter)$
When $Rand1 > P_{pr}$
$F_{sot}^{t+1} = F_{sot}^{t} + d_s \times S_c\left(F_{sht}^{t+1} - F_{sot}^{t}\right)$
else
$F_{sot}^{t+1} = random\ \ position$
end
end
When $Rand2 > P_{pr}$
$F_{snt}^{t+1} = F_{snt}^{t} + d_s \times S_c\left(F_{sot}^{t+1} - F_{snt}^{t}\right)$
else
$F_{snt}^{t+1} = random\ \ position$
When $Rand3 > P_{pr}$
$F_{snt}^{t} = F_{snt}^{t} + d_s \times S_c\left(F_{sht}^{t+1} - F_{snt}^{t}\right)$
else
$F_{snt}^{t+1} = random\ \ position$

end
end
Determine the exploration capacity using Equation (10)
Determine the exploitation capacity using Equation (11)
end

Figure 4 shows the (a) sample of input images and (b) segmentation using FCM-ESSO. It is observed from the Figures that the tumor regions are segmented correctly by the proposed FCM-ESSO.

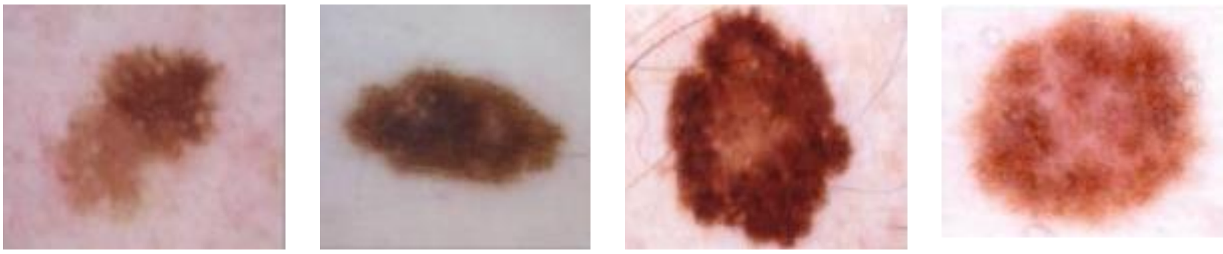

(a)

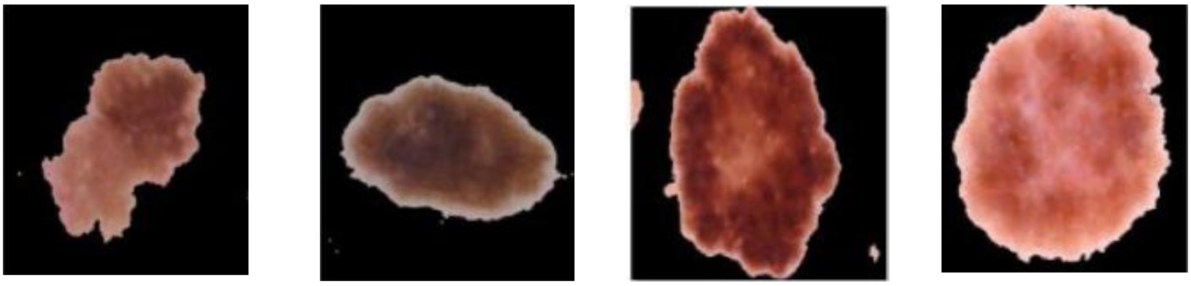

(b)

Fig 4: Qualitative analysis of (a) sample of input images and (b) segmentation using FCM-ESSO

3.4 Feature extraction and classification

Hybrid Inception-residual (I-R) network: This network has residual connections for the blocks of inception. There are three kinds of blocks in this network and they are described as follows:

- *Stem layer:* The input of the pre-processed skin images are given as input to this block and it carries out three 3x3 convolutions. The last stem layer is generated using 3 inception layers. The initial and third inception layer has 2 trails with maxpooling and 3x3 convolutions. Further, the second layer has 2 trails with 1x1 and 3x3 convolutions.
- *Inception-ResNet (I-R) block:* In the inception blocks, the residual connections are provided for avoiding vanishing issues. I-R V2 exploits three kinds of I-R blocks. I-R-A block has three trails with 1x1 and 3x3 convolutions. I-R-B and I-R-C has 2 trails. These two block have same convolutions but the size of convolutional filter is different.
- *Reduction layer:* It utilizes pooling and convolutional trails to reduce the features. Reduction A layer has 1 maxpooling layer and 2 convolutional trails. Reduction A layer has 1 maxpooling layer and 3 convolutional trails.

Further, for improving the performance of the system the network I-R is integrated with the dense network. That is this network is placed between the I-R and softmax layer. This network has 3 dense layers; the initial 2 dense layers has 2,048 neurons and the final layer has 1,024 neurons. Every dense layer has leaky ReLU (LReLU) (regularized linear unit) and dropout layer. Here, the dropout layer is used for reducing the overfitting issue.

Figure 5 presents the structure of Hybrid I-R network which is the integration of I-R network and dense network. It has one stem layer, five I-R-A, ten I-R-B and five I-R-C. Further, it has 1 reduction-A and 1 reduction-B. The output from the five I-R-C is given to the flattened layer and dense network. The integration of dense layers enhances the performance of classification. The weights of ImageNet are initialized in the hybrid I-R network and the learning parameters are discarded for reducing the training time.

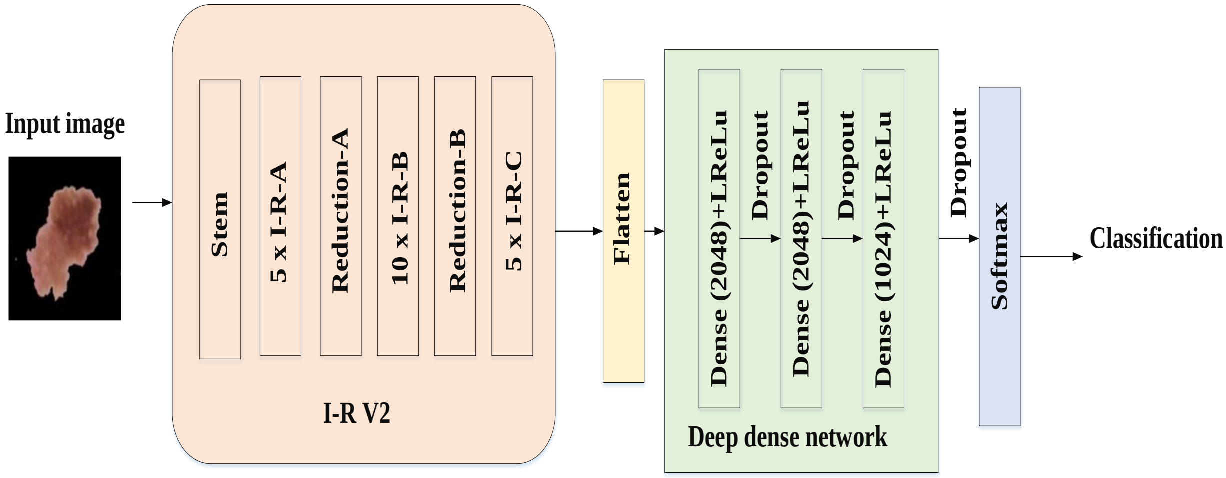

Fig 5: Structure of Hybrid I-R network

The stages to develop the proposed Hybrid I-R network are given below:

Stage 1: Initially, the input image size of I-R V2 is 256x256x3 and it produces 6x6x1536 feature maps.

Stage 2: This multi-dimensionality feature map is flattened for generating a 1D vector with the 1024 features.

Stage 3: At last, a softmax layer having 3 neurons is used for classifying BCC, melanoma and SCC.

In dense layers, the ReLU is utilized as an activation function but the negative process of this activation is 0. Hence, in this work, LReLU is integrated with every dense layer and it is given as:

$$\psi(y) = \begin{cases} y & where \quad y \geq 0 \\ \beta \times y & where \quad y < 0 \end{cases} \qquad (1)$$

LReLU permits negative process and it is given in Equation (1). In this work, the $\beta = 0.3$ is considered for every dense layer for preserving a negative part. The loss function used in this work is cross entropy (CE) and it is expressed as:

$$L_{CE} = \sum_{j=1}^{M} -e_j^{(k)} \log y_j^{(k)} \qquad (1)$$

where $e_j^{(k)}$ is the output vector and $y_j^{(k)}$ is the m^{th} class output vector.

4. Results Analysis

This section presents the experimental analysis of the proposed model that has been provided to the dataset for analyzing the efficiency of the system. The software utilized for the simulation is Python and the configuration of the software is an Intel core 17 with a 47904 processor and 64 GB RAM. Here, the performance of each method is compared with other models on the basis of accuracy, F-score, recall and precision. Further, the confusion matrix and ROC curve are presented. There are four essential parameters which is important for the confusion matrix. Table 2 presents the hyperparameters of the Hybrid I-R network. Adam is the optimizer utilized, the epoch considered are 6, size of batch and learning rate are 100 and 0.1.

Table 2: Hyperparameters of the Hybrid I-R network

Hyperparameter	Value
Number of epoch	6
Size of batch	100
Optimizer	Adam
Learning rate	0.1
Loss	CE

T_p (True positive)- Accurately classified positive samples

T_n (True negative)- Accurately classified negative samples

F_p (False positive)- Incorrectly classified the positive samples

F_n (False negative)- Incorrectly classified the negative samples

Accuracy: It is the ratio of total number of accurate prediction to the entire samples and it is expressed as:

$$A = \frac{T_p + T_n}{T_p + T_n + F_p + F_n} \quad (2)$$

Recall: It is the total of correct positive outcomes splited by the total of positive outcomes achieved by the classifier. It is expressed as:

$$\mathrm{Re} = \frac{T_p}{T_p + F_n} \quad (3)$$

Precision: It is the measure of the total of positive outcomes to the total of each conjugate samples. It is expressed as:

$$P = \frac{T_p}{T_p + F_p} \quad (4)$$

F-score: It is the harmonic mean which is used for balancing the recall and precision. It consider both F_p and F_n for the calculation and works well on the imbalanced data. it is expressed as:

$$F1 - score = \frac{2T_p}{2T_p + F_p + F_n} \quad (5)$$

Figure 6 and 7 show the training and validation losses and accuracies of the proposed Hybrid I-R network. These performances are carried out by 5-fold cross-validation. This network doesn't consider the basic parameters of I-R network; hence it generates high validation and training losses in the initial epochs. Further, it shows high learning because of 3 dense layers and CE loss. The dense layer's parameters are learned in all epochs and use the features of skin cancer. The proposed Hybrid I-R network converges and obtains an optimal loss in 5 epoch values. Very less training and validation losses are achieved at the 5th epoch and high accuracy is achieved for all the epoch values.

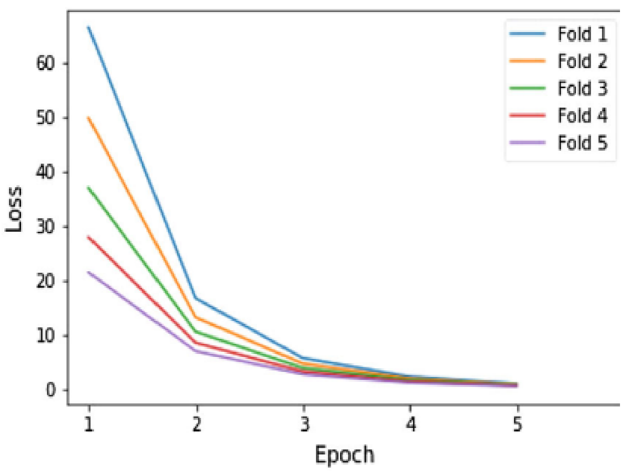

(a)

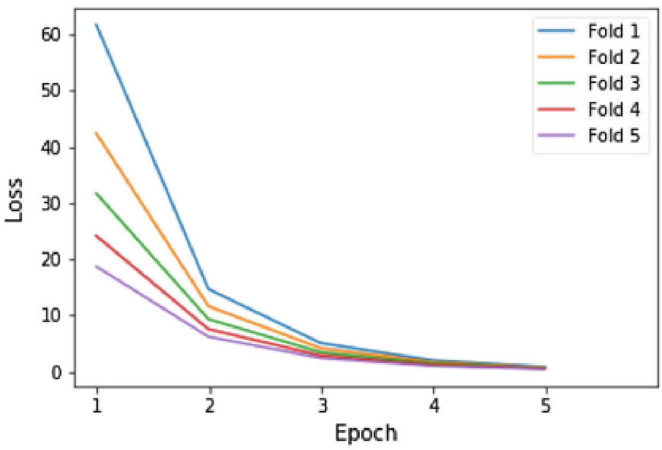

(b)

Fig 6: Training and validation losses of Hybrid I-R network

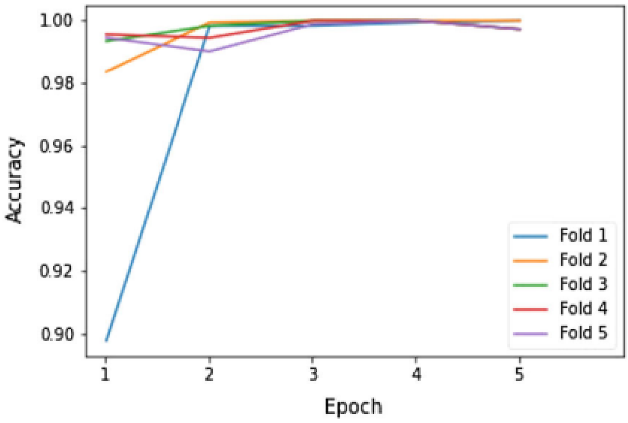

(a)

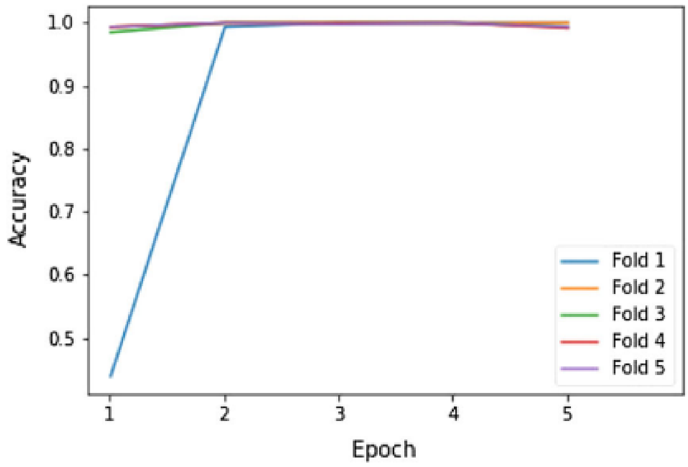

(b)

Fig 7: Training and validation accuracies of Hybrid I-R network

Table 3 shows the performance comparison of various approaches like CNN, Inception, ResNet, AlexNet, DenseNet and Hybrid I-R network (proposed) are compared. Here, the results are compared for various measures. The overall performance is carried out for the m multi-classification. The accuracy and recall values achieved by the proposed Hybrid I-R network is 99.78% and 99.12% on the ISIC dataset.

Table 3: Performance comparison of various approaches

	Methods	Accuracy	Recall	Precision	F-score
With augmentation	CNN	94.23	89.1	94.21	94.9
	Inception	94.41	91.56	93.87	95.0
	ResNet	95.26	92.89	95.17	95.2
	AlexNet	96.23	94.12	96.01	96.3
	DenseNet	97.12	98.34	96.89	97.8
	Hybrid I-R network	99.78	99.12	98.9	99.0

Figure 9 represents the ROC precision-recall curve of the proposed Hybrid I-R network. In Figure 9 (a), the ROC graph is plotted between the true positive rate and specificity values. Here, the AUC value (area under the curve) achieved for the proposed Hybrid I-R network is 0.9909. In Figure 9 (a), the graph is plotted between the precision and recall curves. Here, the AUC value achieved for the proposed Hybrid I-R network is 0.920.

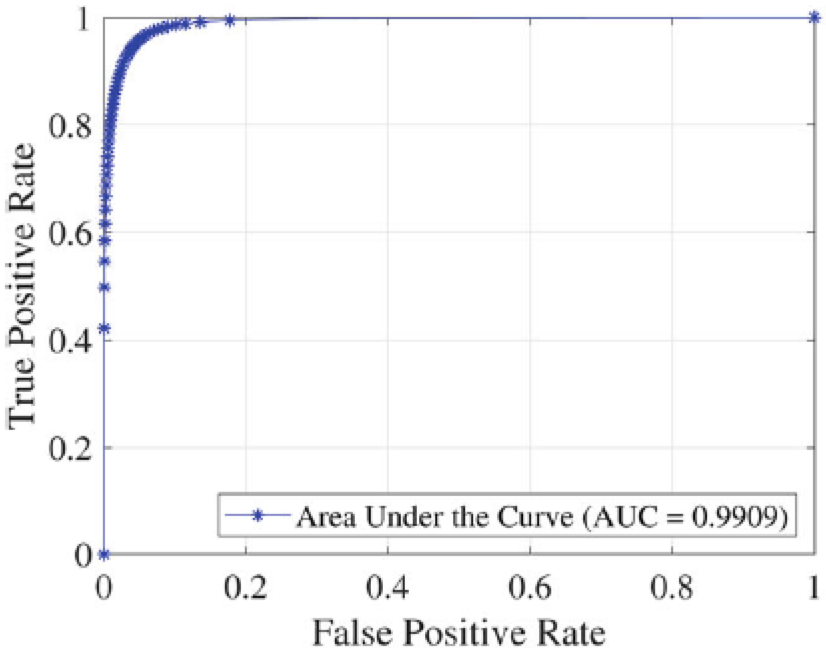

(a)

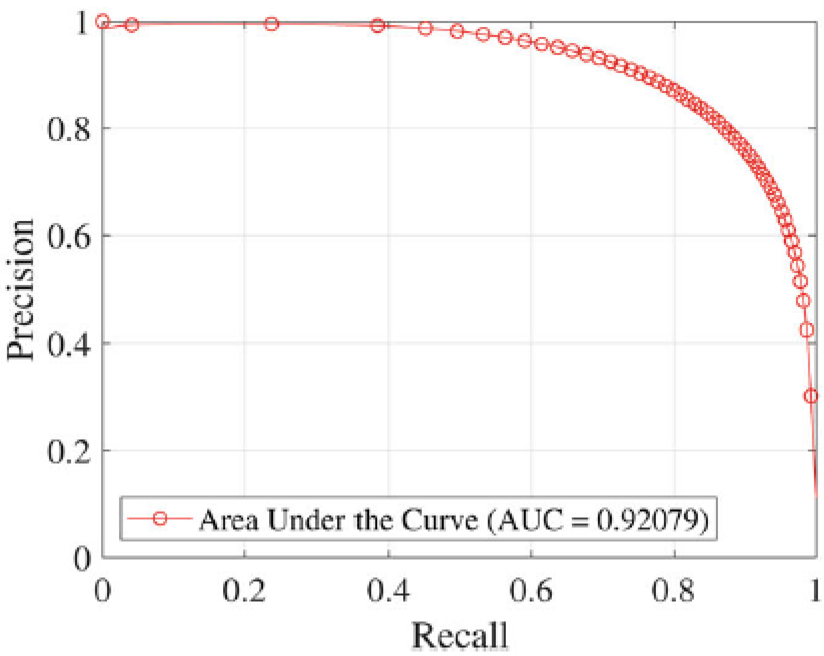

(b)

Fig 9: ROC and precision-recall curve of the proposed Hybrid I-R network

For verifying the effectiveness of the proposed ESSO, the convergence is provided in Figure 10. Here, the performance is carried out by varying the iteration of 100. It is observed that the fitness value of the proposed ESSO is better than the standard SSO. After the 20th iteration, the value of fitness is stable for all iteration.

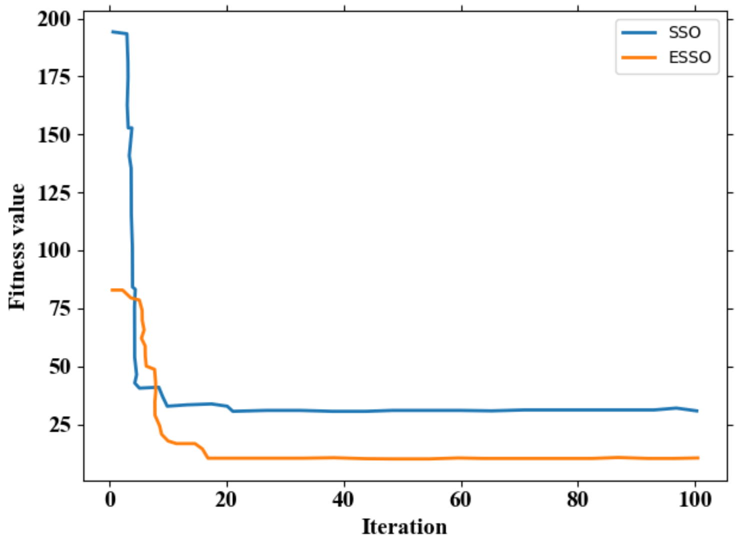

Fig 10: Convergence analysis of the ESSO and SSO

5. Conclusion

This work presented an enhanced DL model based multi-skin cancer classification. This model was presented for detecting and categorizing the presence of skin tumors from dermoscopic images. The major processes like hair removal, data augmentation, feature extraction and classification processes were carried out. Initially, the hair removal and segmentation process was carried out. The DL model Hybrid I-R network was used for extracting and classifying the multi-classification of skin cancer. The overall evaluation was carried out on the ISIC dataset with 5-fold cross-validation. The performances of the proposed hybrid model are compared with the other existing models and achieved better accuracy, recall and precision of 99.78%, 99.12% and 98.9% respectively. In the future, different datasets will be utilized for classifying various types of skin cancer. Further, the DL network will be fine-tuned by some metaheuristic optimization to enhance the performance of the system.

Competing interests: The author's don't have any competing interests.

Funding: No Funding was granted for this research

Availability of data and materials: The authors didn't use any third party data.

Authors' contributions: In this manuscript preparation author 1 and author 2 prepared the concept and author 3 and 4 prepared the implementation part and author 5 prepared the grammatical errors and author 6 prepared the journal formatting.

References

[1] Vimercati, L., De Maria, L., Caputi, A., Cannone, E.S.S., Mansi, F., Cavone, D., Romita, P., Argenziano, G., Di Stefani, A., Parodi, A. and Peris, K., 2020. Non-melanoma skin cancer in outdoor workers: a study on actinic keratosis in Italian navy personnel. International journal of environmental research and public health, 17(7), p.2321.

[2] Leiter, U., Keim, U. and Garbe, C., 2020. Epidemiology of skin cancer: update 2019. Sunlight, Vitamin D and Skin Cancer, pp.123-139.

[3] Sander, M., Sander, M., Burbidge, T. and Beecker, J., 2020. The efficacy and safety of sunscreen use for the prevention of skin cancer. CMAJ, 192(50), pp.E1802-E1808.

[4] Xu, Z., Sheykhahmad, F.R., Ghadimi, N. and Razmjooy, N., 2020. Computer-aided diagnosis of skin cancer based on soft computing techniques. Open Medicine, 15(1), pp.860-871.

[5] Adla, D., Reddy, G., Nayak, P. and Karuna, G., 2021. Deep learning-based computer aided diagnosis model for skin cancer detection and classification. Distributed and Parallel Databases, pp.1-20.

[6] Carrera, E.V. and Ron-Domínguez, D., 2018, August. A computer aided diagnosis system for skin cancer detection. In International Conference on Technology Trends (pp. 553-563). Springer, Cham.

[7] Setiawan, A.W., 2020, February. Effect of Color Enhancement on Early Detection of Skin Cancer using Convolutional Neural Network. In 2020 IEEE International Conference on Informatics, IoT, and Enabling Technologies (ICIoT) (pp. 100-103). IEEE.

[8] Selvarasa, M. and Aponso, A., 2020, March. A Critical Analysis of Computer Aided Approaches

for Skin Cancer Screening. In 2020 International Conference on Image Processing and Robotics (ICIP) (pp. 1-4). IEEE.

[9] Kadampur, M.A. and Al Riyaee, S., 2020. Skin cancer detection: Applying a deep learning based model driven architecture in the cloud for classifying dermal cell images. Informatics in Medicine Unlocked, 18, p.100282.

[10] Wei, L., Ding, K. and Hu, H., 2020. Automatic skin cancer detection in dermoscopy images based on ensemble lightweight deep learning network. IEEE Access, 8, pp.99633-99647.

[11] Le, D.N., Le, H.X., Ngo, L.T. and Ngo, H.T., 2020. Transfer learning with class-weighted and focal loss function for automatic skin cancer classification. arXiv preprint arXiv:2009.05977.

[12] Kumar, S.N. and Ismail, B.M., 2020. Systematic investigation on Multi-Class skin cancer categorization using machine learning approach. Materials Today: Proceedings.

[13] Adla, D., Reddy, G., Nayak, P. and Karuna, G., 2021. Deep learning-based computer aided diagnosis model for skin cancer detection and classification. Distributed and Parallel Databases, pp.1-20.

[14] Ismail, M.A., Hameed, N. and Clos, J., 2021. Deep learning-based algorithm for skin cancer classification. In Proceedings of International Conference on Trends in Computational and Cognitive Engineering (pp. 709-719). Springer, Singapore.

[15] Duggani, K. and Nath, M.K., 2021. A technical review report on deep learning approach for skin cancer detection and segmentation. Data Analytics and Management, pp.87-99.

[16] Chaturvedi, S.S., Tembhurne, J.V. and Diwan, T., 2020. A multi-class skin Cancer classification using deep convolutional neural networks. Multimedia Tools and Applications, 79(39), pp.28477-28498.

[17] Ali, M.S., Miah, M.S., Haque, J., Rahman, M.M. and Islam, M.K., 2021. An enhanced technique of skin cancer classification using deep convolutional neural network with transfer learning models. Machine Learning with Applications, 5, p.100036.

[18] Sedigh, P., Sadeghian, R. and Masouleh, M.T., 2019, November. Generating synthetic medical images by using GAN to improve CNN performance in skin cancer classification. In 2019 7th International Conference on Robotics and Mechatronics (ICRoM) (pp. 497-502). IEEE.

[19] Garg, R., Maheshwari, S. and Shukla, A., 2021. Decision support system for detection and classification of skin cancer using CNN. In Innovations in Computational Intelligence and Computer Vision (pp. 578-586). Springer, Singapore.

[20] Kumar, M., Alshehri, M., AlGhamdi, R., Sharma, P. and Deep, V., 2020. A de-ann inspired skin cancer detection approach using fuzzy c-means clustering. Mobile Networks and Applications, 25(4), pp.1319-1329.

[21] Mijwil, M.M., 2021. Skin cancer disease images classification using deep learning solutions. Multimedia Tools and Applications, 80(17), pp.26255-26271.

[22] Zhang, N., Cai, Y.X., Wang, Y.Y., Tian, Y.T., Wang, X.L. and Badami, B., 2020. Skin cancer diagnosis based on optimized convolutional neural network. Artificial intelligence in medicine, 102, p.101756.

[23] Amin, J., Sharif, A., Gul, N., Anjum, M.A., Nisar, M.W., Azam, F. and Bukhari, S.A.C., 2020. Integrated design of deep features fusion for localization and classification of skin cancer. Pattern Recognition Letters, 131, pp.63-70.

[24] Afza, F., Sharif, M., Khan, M.A., Tariq, U., Yong, H.S. and Cha, J., 2022. Multiclass skin lesion classification using hybrid deep features selection and extreme learning machine. Sensors, 22(3), p.799.

[25] Cassidy, B., Kendrick, C., Brodzicki, A., Jaworek-Korjakowska, J. and Yap, M.H., 2022. Analysis of the ISIC image datasets: usage, benchmarks and recommendations. Medical Image Analysis, 75, p.102305.

[26] Raju, D. Naveen, Hariharan Shanmugasundaram, and R. Sasikumar. "Fuzzy segmentation and black widow–based optimal SVM for skin disease classification." Medical & biological engineering & computing 59, no. 10 (2021): 2019-2035.

[27] Karthik, Ra, Tejas Sunil Vaichole, Sanika Kiran Kulkarni, Ojaswa Yadav, and Faiz Khan. "Eff2Net: An efficient channel attention-based convolutional neural network for skin disease classification." Biomedical Signal Processing and Control 73 (2022): 103406.

[28] Melbin, K., and Y. Jacob Vetha Raj. "Automated detection and classification of skin diseases using diverse features and improved gray wolf-based multiple-layer perceptron neural network." International Journal of Imaging Systems and Technology 31, no. 3 (2021): 1317-1333.